Paper

INFLUENCE OF ROOM GEOMETRY AND VENTILATION RATE ON AIRFLOW AND AEROSOL DISPERSION: IMPLICATIONS FOR WORKER PROTECTION

Jeffrey J. Whicker, Piotr T. Wasiolek, and Rebecca A. Tavani*

Abstract—**Knowledge of dispersion rates and patterns of radioactive aerosols and gases through workrooms is critical for understanding human exposure and for developing strategies for worker protection. The dispersion within rooms can be influenced by complex interactions between numerous variables, but especially ventilation design and room furnishings. For this study, dependence of airflow and aerosol dispersion on workroom geometry (furnishings) and ventilation rate were studied in an experimental room that was designed to approximate a plutonium laboratory. Three different configurations of simulated gloveboxes and two ventilation rates (approximately 6 and 12 air exchanges per hour) were studied. A sonic anemometer was used to measure airflow parameters including all three components of air velocity vectors and turbulence intensity distributions at multiple locations and heights. Aerosol dispersion rates and patterns were measured by releasing aerosols multiple times from six different locations. Aerosol particle concentrations resolved in time and space were measured using 16 multiplexed laser particle counters. Comparisons were made of air velocities, turbulence, and aerosol transport across different ventilation rates and room configurations. A strong influence of ventilation rate on aerosol dispersion rates and air velocity was found, and changes in room geometry had significant effects on aerosol dispersion rates and patterns. These results are important with regards to constant evaluation of placement of air sampling equipment, benchmarking numerical models of room airflow, and design of ventilation and room layouts with consideration of worker safety.**

Health Phys. 82(1):52–63; 2002

Key words: aerosols; ventilation; air sampling; occupational safety

INTRODUCTION

THE LEVEL of worker protection from accidentally released airborne radioactive materials is heavily influenced by the ventilation-driven airflow patterns in a workroom. For example, protective airflow patterns keep airborne concentrations in worker's breathing zones (BZ) low and then rapidly exhaust the material from the room. Further, worker safety is enhanced by the sensitive and timely measurement of the presence and levels of radioactivity in room air. Effective use and placement of air samplers and real-time monitors to measure air quality requires knowledge of prevailing airflow patterns in the room.

Because of the impact of room airflow on worker safety, the Department of Energy (DOE) and the Nuclear Regulatory Commission (NRC) have regulatory guidance documents detailing the rationale and techniques for assessment of airflow patterns in work rooms (U.S. DOE 1999; Hickey et al. 1993). In addition, regulators are aware that the airflow patterns can change over time as room conditions change. Therefore, these guides require periodic evaluations of airflow patterns, and reevaluations after rooms are reconfigured in such a way as to alter airflow patterns.

It is generally accepted that airflow patterns can be affected by dramatic changes in room conditions or from the cumulative effects of smaller changes. However, for compliance and to maintain high levels of worker protection, the following questions should be considered. First, is the time frame for periodic evaluations suggested by the guides (i.e., every 3 y) appropriate for the facility? And second, what types of room changes result in an alteration of airflow patterns that significantly impact worker safety?

Other researchers have shed some light into the issue. Awbi (1991) summarizes a number of studies that explore factors that control room airflow. Buchanan et al. (1995) numerically demonstrated that airflow can be significantly altered with the simple addition of a partition in a room, and that mixing improves as the airflow disruption increases. This disruption depended on the interplay of the obstruction size, shape, and placement relative to airflow. Haghighat et al. (1996) showed that the presence of furniture in an office space completely changed contaminant dispersion and that an increase in the rate of outdoor air supply into the office significantly reduced the mean age of the room air.

Specific to nuclear facilities, Whicker et al. (2000a) used computational fluid dynamics (CFD) modeling of airflow and aerosol dispersion in a plutonium facility to

*Los Alamos National Laboratory, Health Physics Measurements Group, Mail Stop G761, Los Alamos, NM 87545.

For correspondence or reprints contact J. J. Whicker at the above address, or email at jjwhicker@lanl.gov.

(*Manuscript received* 9 *January* 2001; *revised manuscript received* 16 *April* 2001, *accepted* 26 *July* 2001)

0017-9078/02/0

investigate the effects of room configuration and ventilation air exchange rate on continuous air monitor (CAM) response and worker exposure. This work, based on computer simulation, showed that the removal of large sections of glovebox lines had significant effects on local airflow patterns and aerosol dispersion, and that predicted worker exposure was found to be slightly higher at seven room air exchanges per hour than at ten.

Knowledge of the effects of room and ventilation conditions on airflow patterns, which are closely tied to air quality measurements and worker exposure, could be used for better design of room ventilation and CAM placement (Whicker et al. 1999). For example, steep, time-dependent concentration gradients can exist in the vicinity of the release areas (Drescher et al. 1997; Whicker et al. 1997). Also, research has shown that complete mixing can take up to several hours (Buchanan et al. 1995) and under some conditions may not be achievable (Nicas 1996). In conditions of low mixing, workers near the site of release may receive larger exposures, and these exposures can be much greater than that predicted by remote area air samples. In contrast, Flynn et al. (1996) showed that with proper airflow, the concentration in the BZ could be reduced by several orders-of-magnitude. Therefore, proper understanding and consideration of the ventilation system, room layout, and air sample and CAM placement can improve worker safety and exposure assessment.

In the Los Alamos National Laboratory (LANL) plutonium facility, glovebox sections can be added, removed, or modified, and room ventilation rates can fluctuate, so it is important to investigate how changes in these factors can influence general airflow characteristics and aerosol transport. Because of safety considerations, we could not make the necessary measurements inside the plutonium facilities. Therefore, the experiment was carried out in a test facility that was designed to resemble a LANL plutonium laboratory, but whose furnishings, ventilation design, and ventilation rates could readily be reconfigured. The experimental room contained multiple glovebox lines, an overhead trolley (passbox), and a ventilation design with ceiling supply and exhausts near the room corners and close to the floor. The main goals of this study were to investigate the effects of changes in ventilation rates and room furnishings on (1) aerosol dispersion rates and patterns, and (2) airflow characteristics such as velocity, direction, and turbulence intensity.

MATERIALS AND METHODS

Experimental room

The simulated plutonium workroom used in this study is a freestanding structure located within a larger building. The room is a modular metal-wall structure with x, y, and z dimensions of 4.8 × 6.1 × 2.4 m ($V = 70.3$ m^3) and is furnished with two mockup glovebox lines and an overhead passbox (a sealed tunnel used for moving radioactive samples between gloveboxes in a plutonium facility). The mockup gloveboxes and the passbox were made of aluminized foamboard that were easily reconfigured. This allowed us to consider three different configurations: 1) two full rows of gloveboxes and passbox (FB), 2) half of the gloveboxes removed (HB) with the passbox, and 3) all gloveboxes and passbox removed (NB). Schematic cross-sections of the room configurations are presented in Fig. 1a, b, and c.

The room was supplied with 100% re-circulated air using a portable blower.[†] The room supply air was introduced into the room through four 0.2 m-diameter inlets located on the ceiling (Fig. 1), and the supply air was then diffused into the rooms with 0.3-m-diameter horizontal deflector plates that were located about 15 cm below each supply inlet. The room air was then exhausted through four 0.2-m-diameter adjustable flow exhaust registers located in the room corners, 0.3 m above the floor. The exhausted air was passed through a high efficiency particulate air (HEPA) filter to remove exhausted particulate and then reintroduced back into the room. The nominal room air exchange rate was set to either approximately 6 h^{-1} (LV) or 12 h^{-1} (HV) by adjusting the baffle plate on the air-blower outlet line. Measurements of the volumetric flow rate at the inlet and outlet registers were made using commercial instrumentation[‡] and yielded the average values presented in Table 1. A near-uniform distribution of air velocities around the deflector plates was verified by measurements with a hot wire anemometer[§] around the edge of the deflector plates. Because the experimental room is located indoors with a thermally insulated floor, there was no significant temperature gradient (less than 0.5°C) detected between opposite walls (including ceiling and floor), as measured with fine wire thermocouples[‖]. The room openings (e.g., sampling or cable ports) were sealed to make the structure as air tight as possible.

Aerosols measurements

The methodology used in the present aerosol study is similar to the one described in Whicker et al. (1997). Because most releases that occur in LANL workrooms are acute "puff" releases, our study focused on short-duration releases (60 s). In addition, the data analysis in the present study emphasized the time-dependent nature of aerosol dispersion. The time resolution of concentration measurements in this study was 10 s. This resolution allowed analyses of the time progression of aerosol dispersion.

To simulate an accidental release, polydisperse Dioctyl Sebacate (DOS) oil aerosols were generated using a custom-made orifice nozzle. Operation of the nozzle was adjusted so that the released aerosol exited the nozzle with low velocity (approximately 1 cm s^{-1}) and quickly accommodated to local airflow conditions. The

[†] Model SP-700, Radiation Protection Systems, 10 Vista Drive, Old Lyme, CT.

[‡] Model CFM-88-1, Shortridge Instruments, Scottsdale, AZ.

[§] Model 630, Sierra Instruments, Carmel Valley, CA.

[‖] Model FW05, Campbell Scientific, Inc. Logan, UT.

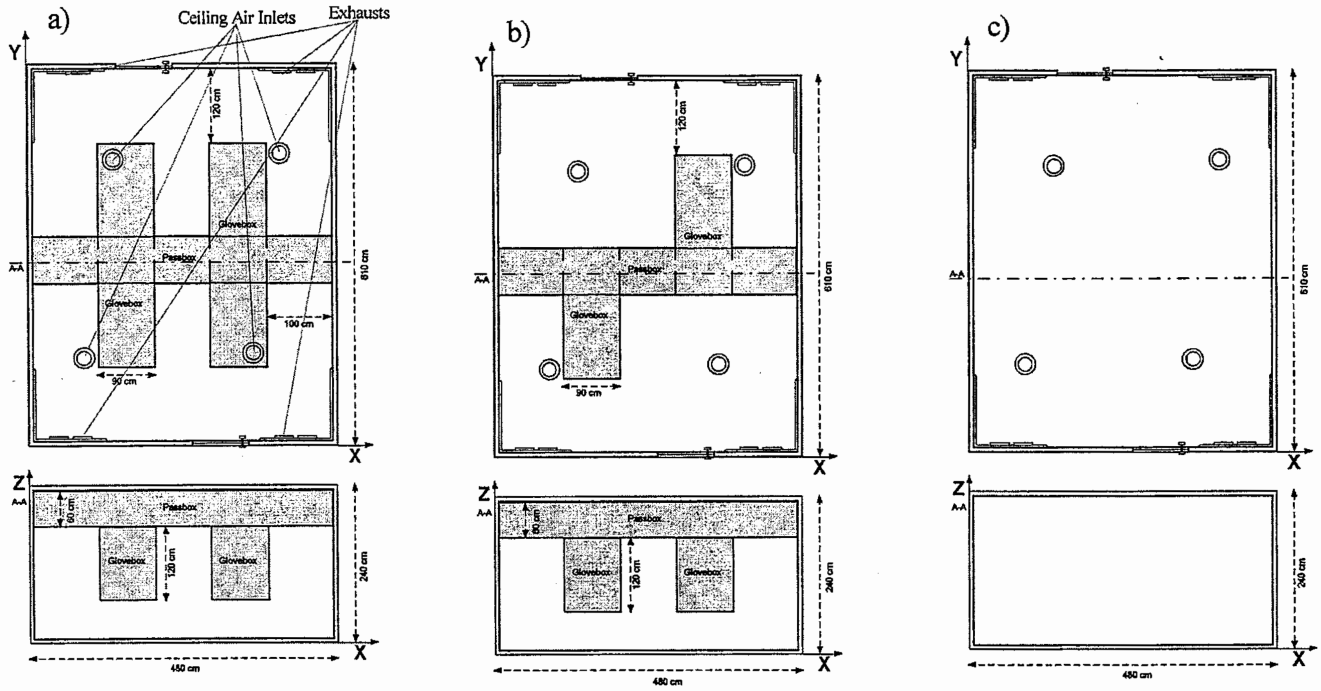

Fig. 1. Schematic diagram of the test-room facility with three different configurations of simulated gloveboxes: a) full set of gloveboxes (FB); b) half set of gloveboxes removed (HB); c) no gloveboxes (NB).

Table 1. Volumetric flow rate at inlet and outlet registers.

	Inlet ($\times 10^{-3}$ m^3 s^{-1})		Outlet ($\times 10^{-3}$ m^3 s^{-1})	
Location	Low ventilation	High ventilation	Low ventilation	High ventilation
SW	30.4 ± 3.3	55.9 ± 0.9	32.6 ± 1.2	60.1 ± 0.7
SE	29.2 ± 1.8	56.0 ± 2.4	37.0 ± 1.9	68.6 ± 0.4
NE	34.9 ± 6.0	76.1 ± 2.4	30.8 ± 2.7	60.9 ± 0.5
NM	31.4 ± 2.2	64.4 ± 0.3	29.5 ± 1.7	63.4 ± 0.4
Total	126.0	252.0	130.0	252.9

particle size distribution was approximately log-normal with a count median diameter of 0.52 μm and a geometric standard deviation of 2.0. Given these sizes, gravitational settling would be minimal and the particles would primarily follow the airflow movement (Hinds 1982).

From an analysis of historical accident data it was concluded that most releases took place as a result of some worker action, and not random events. Therefore, the aerosol release nozzle was positioned 120 cm above floor (the height of glovebox gloves) to simulate a glovebox-glove-failure type release, which is the most common cause of airborne releases (Whicker 1993).

An array of sixteen laser particle counters¶ (LPCs) was established in the test room to make aerosol measurements resolved in time and space. Fig. 2 shows the aerosol release and LPC locations in the experimental room. The LPCs were suspended at 120 cm above the room floor. Location and height of LPCs were selected to be the height of a breathing zone of a worker at the simulated glovebox workstations. The airflow rate of an LPC was controlled by a critical flow orifice with a sampling rate of about 50 cm^3 s^{-1}. All LPCs were coupled to a multiplexer# and the raw data were recorded every 10 s using commercial software.** Raw concentration data were corrected for LPC-specific airflow rates and for particle coincidence counting. A 60-s release was repeated three times at every location, and the averages calculated and analyzed.

For this study, the lag time and dilution was used as the metric for comparison between changes in the ventilation rates and room configurations. The lag-time was defined as the time from the start of the release until the time that an aerosol concentration at sample location

¶ Models 3755 and 7550, Particle Measuring Systems, 5475 Airport Blvd, Boulder, CO.

Model 3701, TSI Inc., 500 Cardigan Road, St. Paul, MN.

** Model 390040 Advanced Cleanroom Software, TSI Inc., 500 Cardigan Road, St. Paul, MN.

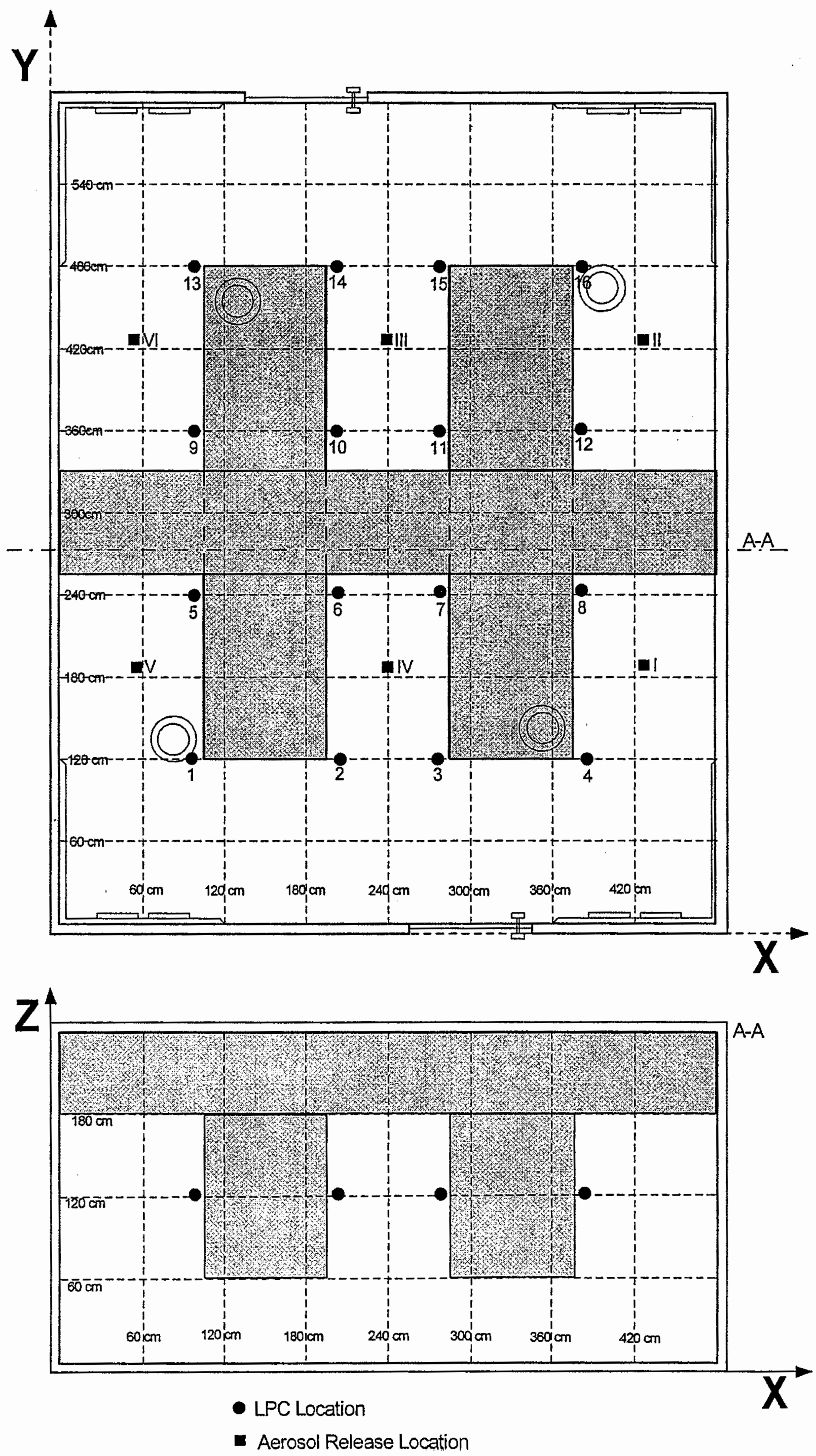

Fig. 2. Location of aerosol releases (Roman numerals) and laser particle counters (LPCs) in the experimental room.

exceeded three standard deviations above background on two consecutive 10-s measurements. The peak concentration was the highest aerosol particle concentration measured during any 10-s sampling period. Using this measurement, the concentration ratio for any individual sampling location [$CR(i)_{peak}$] was calculated as the ratio of the largest mean peak concentration [$C'_{peak(largest)}$] measured in the room divided by each of the mean peak concentrations (averaged over the same three releases) measured at the other sampling locations $C'(i)_{peak}$ as shown in eqn (1):

$$CR(i)_{peak} = \frac{C'_{peak(largest)}}{C'(i)_{peak}}. \quad (1)$$

Also, to evaluate longer-term room mixing, the concentration ratio of the 20-min averaged concentrations [$CR(i)_{20\text{-min}}$] was calculated as the quotient of the largest 20-min average concentration $C_{20\text{-min(largest)}}$ divided by the 20-min averaged concentration measurements made at each individual sampling location [$C(i)_{20\text{-min}}$] as shown in eqn (2):

$$CR(i)_{20\text{-min}} = \frac{C_{20\text{-min(largest)}}}{C(i)_{20\text{-min}}}. \quad (2)$$

Air velocity measurements

A fundamental understanding of aerosol dispersion requires information on the airflow characteristics that transport the particles. Therefore, a commercial sonic anemometer[††] was used to characterize the airflow under the varying conditions. To measure air velocity on each axis, two ultrasonic signals are pulsed in opposite directions across a 10-cm propagation path length and the times-of-flight of the first signal (out) and the second signal (back) are measured and air velocity calculated from the time difference. From these measurements the three orthogonal air velocity components are determined with a programmable sampling rate that can be set from 1 to 60 Hz. A detailed description of air velocity measurements in rooms using sonic anemometry is presented in Wasiolek et al. (1999a) and its use for measurements in the LANL plutonium facility were described by Whicker et al. (2000b). Because air velocities were expected to be low, custom calibration and instrument adjustments were performed in the manufacturer's wind tunnel facility. The results of this custom calibration yielded average threshold velocity values of 0.2 cm s^{-1} at 21° C for all three velocity-vector components. The accuracy of several sonic anemometers, including the model used in this project, was evaluated by Vogt (1997). According to these wind tunnel studies, the average difference between measured values and the reference wind speed values was −1.1%. The minimum and maximum difference between the measured wind speed and the reference tunnel speed for all tested wind speeds and angles of attack were −10.3% and +6.0%, respectively.

The sonic anemometer head was mounted on a mobile cart for ease of transport and leveled after every change in sampling location. The mounting arrangement allowed for adjustment of sampling height. The sonic anemometer head (Vogt 1997) and the mobile cart were designed to minimize local airflow disturbance.

The sampling frequency of the sonic anemometer was set to 1 Hz, and data were collected over a sampling interval of 600 s. The raw, binary data files containing air velocity for each individual directional component were converted to ASCII text format, corrected for offset, and rotated to align orientation of the sonic sampling head with room coordinates.

The 19 locations marked in Fig. 3 were selected for air velocity measurements. Because the experimental room had a ceiling-mounted passbox in two of the gloveboxes' configurations, the sampling heights varied depending on location. At locations 7, 8, and 9, measurements were made from only the two sampling heights of 60 and 120 cm above the room floor, whereas for all remaining sampling locations the sampling heights were approximately 60, 120, and 180 cm. In the NB room configuration, all three heights at each of 19 area locations were sampled. The sonic anemometer was positioned 50 cm from glovebox faces and the room walls. Measurements were performed under steady-state conditions, which were established by waiting at least 5–10 min (one nominal air exchange) after closing and sealing the room door.

Changes in airflow direction were measured by the angle between the flow vectors for each ventilation/room geometry condition. Flow vectors for each sampling location were paired with the flow vector at the same location but measured under either a different ventilation rate (same room configuration) or a different room configuration (same ventilation rate). The change in direction can be thought of as the angle between these two flow vectors. The angle in radians was determined by

$$\cos^{-1}\theta = \frac{x_1x_2 + y_1y_2 + z_1z_2}{\sqrt{x_1^2 + y_1^2 + z_1^2} \times \sqrt{x_2^2 + y_2^2 + z_2^2}}, \quad (3)$$

where x, y, and z are the velocities in the respective three-dimensional directions.

Turbulence measurements

As described by Stull (1988), a statistical measure of the variability of the air velocity (u') about mean velocity ($\bar{u}$) is the unbiased variance σ_u^2. The standard deviation is interpreted as a measure of the magnitude of the spread or dispersion of the original data from its mean, and it can be used as a measure of the level of turbulence. The level of turbulence might be expected to depend on the mean wind speed, so it is often normalized to the air velocity. There are several different definitions of turbulence intensity used in the literature (Hanzawa et al. 1987; Yost and Spear 1992; Heber and Boon 1993). We chose the more common

[††] Model CSAT3, Campbell Scientific, Inc., Logan, UT.

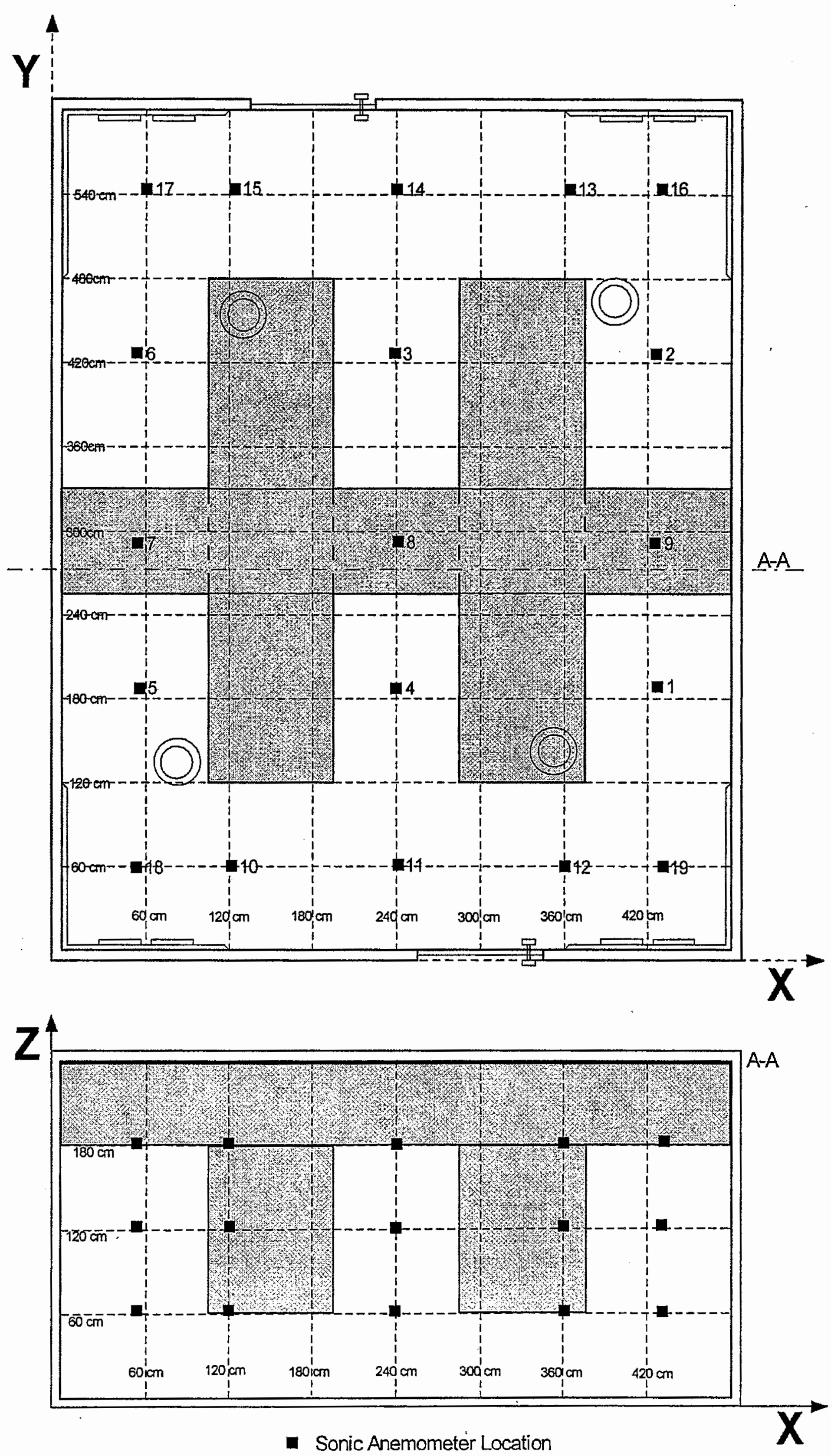

Fig. 3. Location of sonic anemometer measurements in the experimental room.

definition in Hanzawa et al. (1987). They defined turbulence intensity (TI) as the standard deviation (σ) of air velocity (u) divided by local mean velocity, $\bar{u}$, as in eqn (4):

$$\mathrm{TI} = 100\% \frac{\sigma}{\bar{u}}. \quad (4)$$

Data analysis

The metrics of lag time, concentration ratio, air velocity, airflow direction, and turbulence intensity were stratified by ventilation and room configuration. Distributions of these metrics were analyzed for normality using the χ^2 test and the Kolmogorov-Smirnov test (STATISTICA 1994) and homogeneity of variances was tested with the F-test (Remington and Schork 1970) and the Levene test (STATISTICA 1994). Except for the turbulence intensities, none of the above metrics were normally distributed, and the variances of the turbulence intensities were not completely homogeneous. Therefore, statistical comparisons of the effects of ventilation and room configuration on air velocities, turbulence intensities, lag times and their coefficient of variation (COV), and concentration ratios were made using the non-parametric Wilcoxon matched pairs test (STATISTICA 1994).

Histograms of the changes in airflow direction as ventilation rate changed (holding the room configuration constant) and as room configuration was altered (holding the ventilation rate constant) were made to measure the effects of each of the variables.

RESULTS

Room geometry and ventilation rate effects on lag time

One of the primary objectives of the study was to obtain data in regard to transport times of aerosol across rooms. The transport time is the critical parameter for determining response time of CAMs to accidental releases. Table 2 lists the mean lag times for all release locations (Fig. 2) under each of the room and ventilation conditions. Fig. 4 shows distributions of the individual lag time measurements under each of the conditions. In

Table 2. Summary of the lag times and concentration ratios versus aerosol release location for different glovebox configurations and ventilation rates.

FB-LV				FB-HV			
Release location	Lag time mean (s) ± SEM	Mean $CR_{20\text{-min}}$ ± SEM	Mean CR_{peak} ± SEM	Release location	Lag time mean (s) ± SEM	Mean $CR_{20\text{-min}}$ ± SEM	Mean CR_{peak} ± SEM
I	223 ± 24	27 ± 8	69 ± 21	I	71 ± 10	6 ± 1	18 ± 5
II	135 ± 20	13 ± 4	14 ± 4	II	63 ± 8	3 ± 0.4	10 ± 2
III	159 ± 24	26 ± 9	66 ± 26	III	71 ± 9	4 ± 1	16 ± 4
IV	83 ± 10	4 ± 1	20 ± 5	IV	88 ± 11	9 ± 2	52 ± 15
V	123 ± 20	11 ± 3	42 ± 13	V	79 ± 10	8 ± 2	22 ± 7
VI	187 ± 28	33 ± 10	85 ± 26	VI	78 ± 10	9 ± 2	22 ± 6
Avg:	152	19	49	Avg:	75	7	23
SD	49	11	29	SD	9	3	15

HB-LV				HB-HV			
Release location	Lag time mean (s) ± SEM	Mean $CR_{20\text{-min}}$ ± SEM	Mean CR_{peak} ± SEM	Release location	Lag time mean (s) ± SEM	Mean $CR_{20\text{-min}}$ ± SEM	Mean CR_{peak} ± SEM
I	156 ± 23	12 ± 3	69 ± 20	I	75 ± 8	6 ± 1	17 ± 5
II	91 ± 13	6 ± 1	13 ± 3	II	58 ± 7	4 ± 0.4	16 ± 3
III	109 ± 11	4 ± 1	12 ± 4	III	58 ± 6	3 ± 0.4	7 ± 2
IV	115 ± 16	8 ± 2	44 ± 13	IV	76 ± 9	10 ± 2	60 ± 19
V	121 ± 15	7 ± 1	13 ± 3	V	76 ± 9	9 ± 2	28 ± 7
VI	149 ± 16	4 ± 1	14 ± 4	VI	94 ± 12	5 ± 1	14 ± 3
Avg:	124	7	28	Avg:	73	6	24
SD	25	3	24	SD	13	3	19

NB-LV				NB-HV			
Release location	Lag time mean (s) ± SEM	Mean $CR_{20\text{-min}}$ ± SEM	Mean CR_{peak} ± SEM	Release location	Lag time mean (s) ± SEM	Mean $CR_{20\text{-min}}$ ± SEM	Mean CR_{peak} ± SEM
I	130 ± 14	7 ± 1	30 ± 7	I	61 ± 7	6 ± 1	26 ± 6
II	105 ± 10	4 ± 0.4	19 ± 3	II	58 ± 6	3 ± 0.3	8 ± 1
III	91 ± 9	3 ± 0.2	14 ± 3	III	52 ± 5	2 ± 0.2	6 ± 1
IV	88 ± 6	2 ± 0.2	9 ± 2	IV	51 ± 5	2 ± 0.2	4 ± 1
V	179 ± 14	5 ± 1	10 ± 2	V	83 ± 6	5 ± 1	14 ± 2
VI	114 ± 11	3 ± 1	5 ± 1	VI	71 ± 6	3 ± 0.4	10 ± 2
Avg:	118	4	15	Avg:	63	4	11
SD	34	2	9	SD	12	2	8

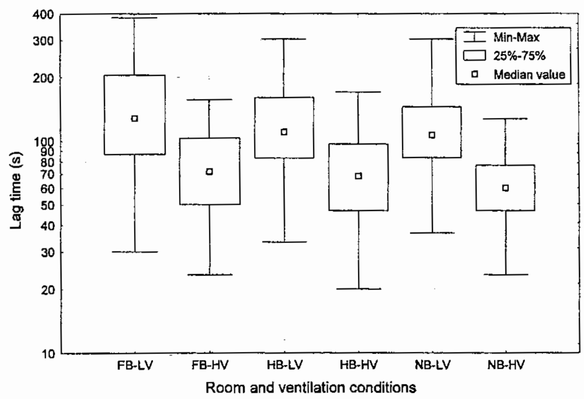

Fig. 4. Distributions of aerosol lag times for the various room configurations and ventilation rates.

all cases, the statistical paired comparison showed that the lag times under the high ventilation rate (holding the room configuration constant) were significantly shorter compared to the lower rate. The results, as summarized in Table 2, show that the two-fold increase in ventilation rate resulted in the decrease of the mean lag time by a factor of 2.0, 1.7, and 1.9 for FB, HB, and NB configurations, respectively.

With regards to room configuration, the individual lag times generally decreased with the removal of the furnishings. The only exception to this finding was between the HB-HV and NB-HV configurations, which were not significantly different. Fig. 4 shows that while the effects of room configurations were significant, the effects were not as dramatic as that found with the change in ventilation rate.

These findings provide additional data for revision of some common assumptions sometimes used for exposure assessment such as the instantaneous mixing of particulate air pollutants or the times needed for evacuation of a contaminated facility. Measurement of the lag times is important for positioning of early warning instruments like CAMs. For example, the level of exposure to workers could be significantly less for good CAM placement if the aerosol cloud reaches the CAM in tens of seconds compared to hundreds of seconds for CAMs that are not positioned well. There was also a strong dependence of average lag time on the release location. For example, for the FB-LV release at location III the average lag time was 83 s, vs. 223 s for release at location I.

Room geometry and ventilation rate effects on dilution

The concentration ratio is a measure of the amount of the released material that gets to the air samplers. Less aerosol dilution between the area around the release location and the air sampler results in more sensitive sampling. Table 2 shows the mean concentration ratios for both the 20-min averaged concentrations and the peak concentrations, and Fig. 5 shows the distributions of the individual measurements. The statistical analysis found significant effects of room configuration on dilution. That is, adding room furnishings increased the dilution of the aerosol in the room. However, with regards to changes in ventilation rate, only the comparison between the FB-LV and the FB-HV showed significantly different concentration ratios.

The influence of room configuration and ventilation rate on the spatial dispersion (mixing) patterns was studied in more detail by comparing the variation of lag times across all sampling locations for each release. Fig. 6 shows the effects of room configuration and ventilation rate on the COV of mean lag times as measured across all LPCs in the room for each release location. The COV was calculated as the standard deviation of the mean lag times divided by the mean lag times. Statistical comparisons showed that there was a significant decrease in the COVs as glovebox lines were removed. We found no significant differences in the COV when only the ventilation rate was varied but the room configuration was the same. This is further evidence that suggests that aerosol mixing throughout the room is less with the increasing addition of large furnishings in the room (i.e., greater dilution).

Room geometry and ventilation rate effects on airflow

Fig. 7a and b shows the mean air velocities for the different configurations and at different measurement heights. The fastest air velocities were measured at the highest locations in the room. This was expected because the supply diffusers were located on the ceiling. The most pronounced height effect was for the FB configuration where the average velocity at 60 cm was only 53% and 57% of that at 180 cm for LV and HV, respectively. In the NB configuration the reduction was only by 31% and 29%. The smaller change in air velocity vertical profile for NB vs. FB and HB configurations shows the influence of obstacles in the room on air velocity field.

Also, Figs. 7a and 7b show that the average air velocities for different configurations scaled up with increased ventilation rate with mean velocities for the low ventilation condition ranging from about 3 to 5 cm s^{-1}, while they ranged from about 7 to 12 cm s^{-1} for the high ventilation conditions. The increase in mean flow velocities between low and high ventilation rates were by factors of 2.71, 2.83, and 2.41 for full set of gloveboxes (FB), for half gloveboxes removed (HB) and for empty room (NB), respectively.

Statistical comparisons showed mean velocities for the high ventilation rates were significantly higher than those measured for the low ventilation rates, and this trend was found for each of the three room configurations. Further, the results showed that changes in room configuration for a constant ventilation rate resulted in no significant differences except for the comparison between the HB-LV and the NB-LV conditions, where the mean velocities for the NB-LV condition was significantly higher.

Fig. 8 shows the effects of variations in room geometry (Fig. 8a) and ventilation rates (Fig. 8b) on the

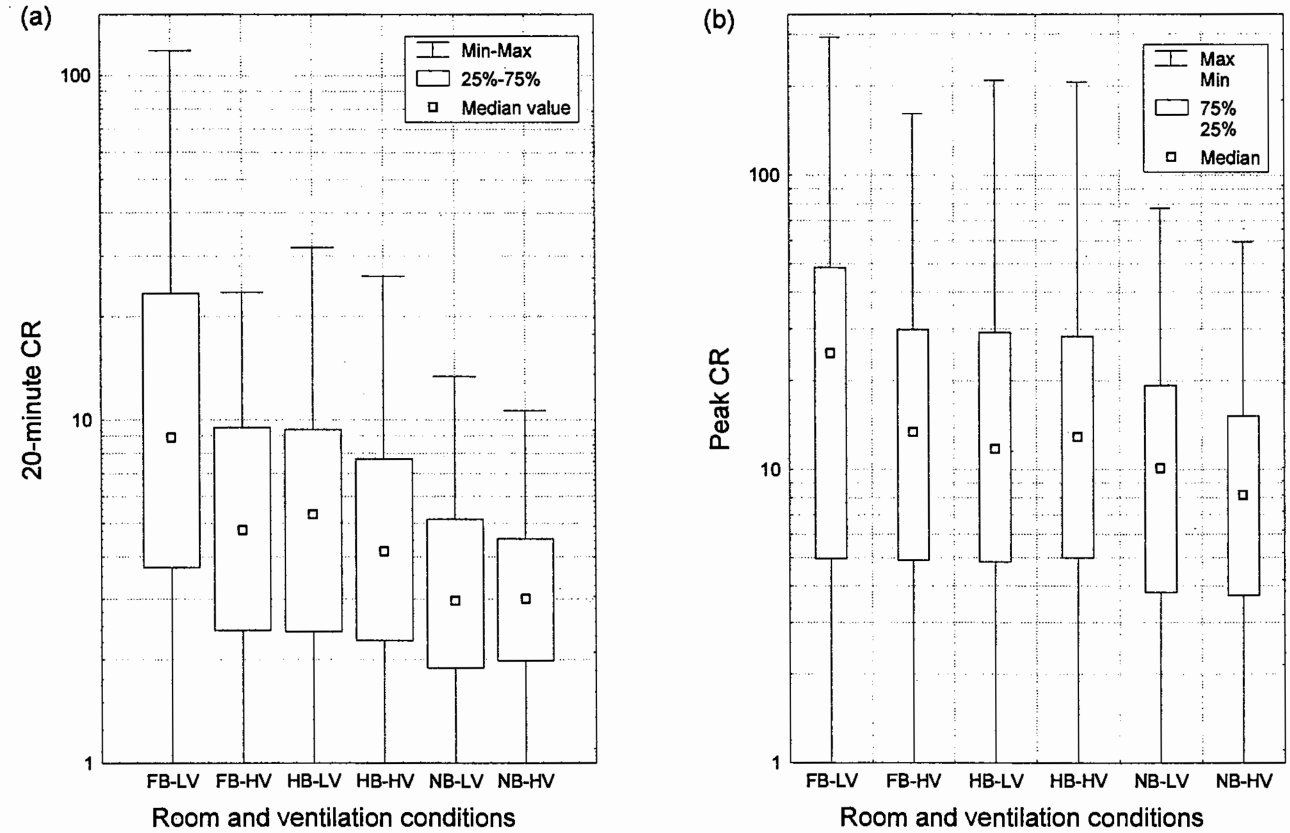

Fig. 5. Distributions of peak and 20-min concentration ratios (CR) for the various room configurations and ventilation rates.

mean direction of airflow as calculated using eqn (3). These histograms show that changes in direction were mostly less than 90° (1.57 radians) across the variations. The median change in angle over the variation in air exchange rate was 0.94 radians (54°) with a quartile range of 0.6 (34°) to 1.4 radians (80°). The median change in direction for variations across changes in room

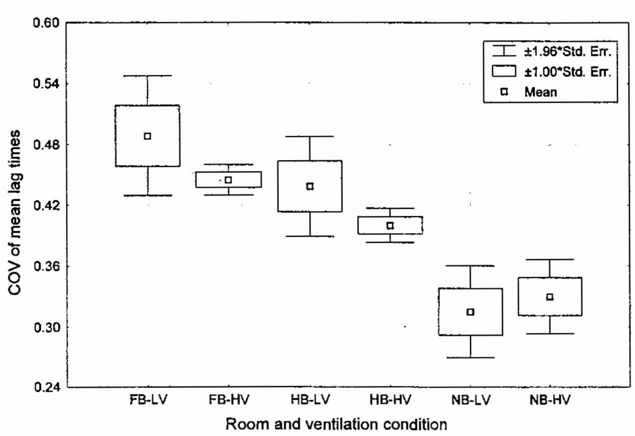

Fig. 6. Coefficient of variation of mean lag times categorized by different glovebox configuration ventilation rates.

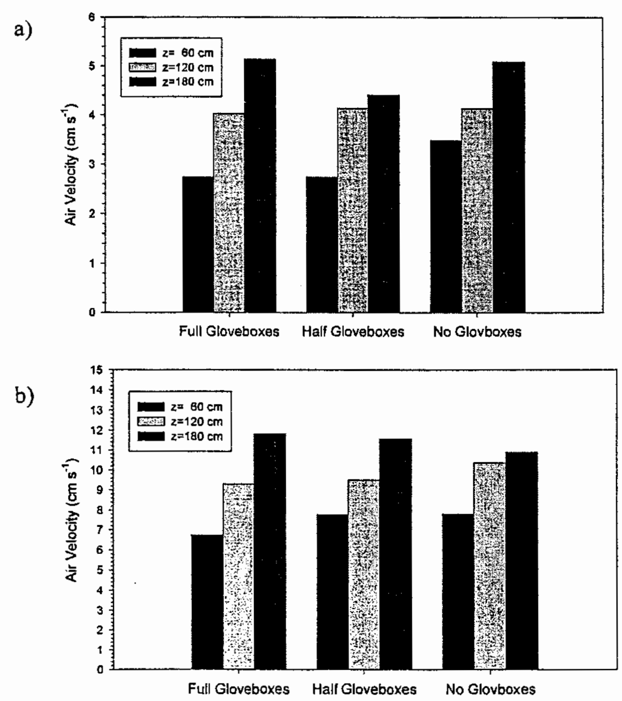

Fig. 7. Vertical air velocity profiles for different room configurations and ventilation rates: a) low ventilation; b) high ventilation.

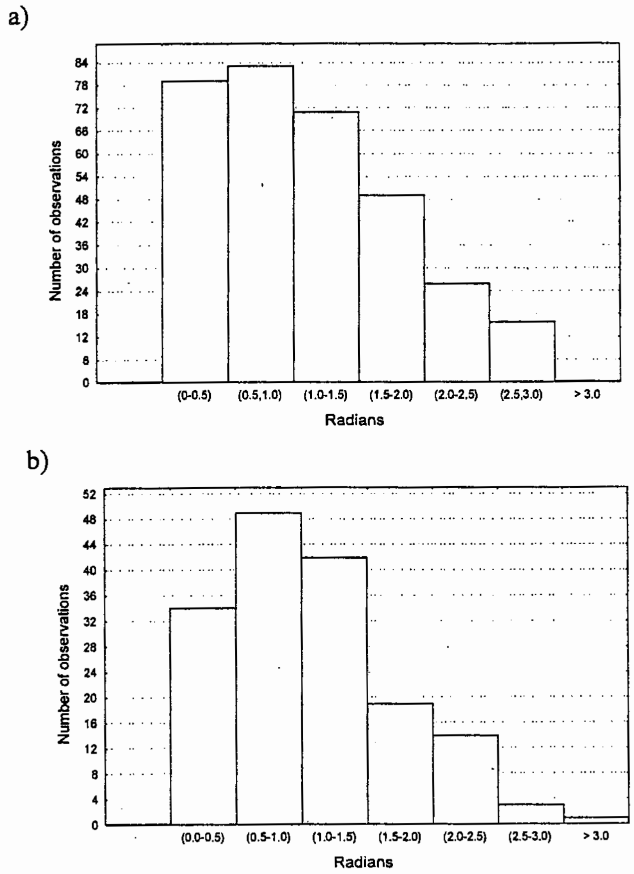

Fig. 8. Changes in airflow direction with changes in: a) glovebox configuration; b) ventilation rate.

configuration was 0.92 (53°) radians with a quartile range of 0.47 (27°) to 1.54 radians (88°). Results of relative changes in flow direction below 90°, independent of ventilation rate and room configuration, suggest that the room flow pattern was predominantly controlled by ventilation supply diffuser design and exterior walls and less by interior room geometry. However, while overall changes in the whole room did not change much, there were individual cases where we found significant changes in airflow direction in areas closest to altered glovebox lines.

The average values of TI were very similar across all configurations and ventilation rates and the individual measurements were normally distributed. The mean TIs ranged from 33% to 39%. Statistical comparisons (using the Wilcoxon matched pairs test) between the turbulence intensities (TI) among the various room and ventilation configurations confirmed that the TIs were generally the same. However, we found that the TI for the NB-LV was significantly less than the NB-HV and the FB-LV conditions. As seen in eqn (4), the result that the TI remained relatively constant, even though the air velocities fluctuated significantly, showed that the standard deviation of the velocity changed in proportion to the mean velocity. An important conclusion from this is that at greater air velocities aerosol transport in the room is also increased. This is due not only from the greater air velocity, but also increased turbulent diffusion.

Finally, while the results of air velocity measurements for different ventilation rates and test-room geometry are summarized in this paper, they are presented in detail in Wasiolek et al. (1999b). The tables in Wasiolek et al. (1999b) include sampling location, individual components of the air velocity vectors u_x, u_y, u_z in cm s^{-1}, absolute velocity, turbulence intensity, and the turbulence intensity of individual components in the x, y, and z directions. Considering the rather simple room geometry and lack of extreme thermal effects in our test facility, this detailed data set may be useful for CFD model benchmarking.

DISCUSSION

The objective of the study was to investigate how the changes in room geometry and ventilation rate influence airflow and aerosol dispersion. Changes in these variables occur quite often in many research facilities that contain toxic materials. Therefore, studying their effects on airflow and aerosol dispersion is important when evaluating the worker exposure, placement of air monitors, and for accurate interpretation of air sample results under varying conditions.

We found that ventilation rate (for the same room configuration) significantly affected lag times and airflow velocities, but had little effect on turbulence intensity. As ventilation rates increased, the lag times decreased, which is likely tied directly to the increase in airflow velocities. The rate that aerosols were transported through the rooms also was affected by turbulent eddies. We found that as mean airflow velocities increased, the deviations of the velocities also increased proportionally. This resulted in the relatively constant turbulence intensity across all strata of ventilation rate and room configuration. This suggests that the rate of aerosol dispersion, as reflected by the lag time, is affected by both the convective airflow velocity in a room and also the turbulent diffusion rate. This confirms the findings of Siurna and Bragg (1986) who showed that the velocity and turbulence fields are of fundamental importance in contaminant dispersion by mechanically ventilated rooms. Finally, changes in ventilation rate, while affecting airflow velocities, did not seem to completely alter the direction of the airflow. We found that over 75% of the changes in direction were less than 1.4 radians (80°) when changes in ventilation alone were considered.

The results also suggested that changes in the room configuration (for the same ventilation rate) had significant effects on the mean lag times, COV, and concentration ratios, but generally had little effect on the direction of the airflow vector, mean airflow velocities, or the turbulence intensity. In general, there was a trend for lag time to decrease with removal of the mock glovebox sections. The data suggest that room structure could slow down aerosol mixing in a room by creating local eddies or air pockets. Removal of the furnishings allows the aerosol to mix more rapidly. Changes in room configuration had no significant effect on airflow velocities, except between HB-LV and NB-LV experimental setup where the HB-LV resulted in lower velocities. It is not clear whether this was due to experimental uncertainty or perhaps to the presence of the structure in the room, which may have altered the local velocities.

It is also possible that there is an effect not only due to adding structure in a room, but also of the placement of the structure relative to the airflow direction and velocity. This effect was suggested by Buchanan et al. (1995) who found an increase in mixing with increasing airflow disturbance. However, the effects of room furnishings and airflow characteristics on worker exposure are complex. Flynn et al. (1996) found that under certain airflow conditions the presence of an object could impede contaminant removal from the breathing zone of a worker. However, if the airflow was from the side of a worker and swept the airborne material out of the space between the worker and the furnishing, the concentrations in the breathing zone were reduced by orders-of-magnitude.

The results of this study demonstrate the importance of having ventilation designs that create airflow to keep inhalation risks to a minimum. For example, ventilation that supplements confinement structures by providing directed airflow into gloveboxes and chemical hoods has proved to be a valuable tool in preventing inadvertent releases. However, there are occasions where these engineering controls have not been sufficient to prevent accidental releases into the interior of rooms where workers might be. For these cases, ventilation that sweeps the released aerosol out of the BZ (especially that of the nearest worker), quickly dilutes it, and then exhausts it from the room is desired.

Further, our results show that there can be steep concentration gradients in a room and lag times are sufficiently long that one should consider these when placing air samplers and CAMs. To determine placement of air samplers and CAMs, quantitative methods (i.e., tracer methods such as that used in this study) or qualitative methods (i.e., smoke studies) can be used. Historically, smoke studies are most commonly used. However, smoke study methods, which are detailed in NUREG-1400 (Hickey et al. 1993), cannot provide the quantitative measurements to accurately answer either how fast the aerosol travels nor how much aerosol gets to the CAMs or retrospective air samplers. In contrast to smoke studies, the employed tracer methods in this study do provide important measurements useable for selecting the number and placement of air samplers and CAMs (Rodgers et al. 1998; Whicker et al. 1997).

Although determining CAM placement in the mock-up facility was not a goal of this study, the results suggest that for conditions where there is better mixing, e.g., higher ventilation rates and more open space in a room, fewer CAMs might be needed and their exact placement less rigorous. While rapid mixing into a room could lower doses, especially for workers closest to the release point, mixing dilutes the aerosol. Therefore, it is important to use CAMs that are as sensitive as possible and their placement be optimal.

CONCLUSION

In conclusion, the results demonstrate that airflow characteristics are altered by large changes in ventilation rates (doubling) or after changes in large structures in a room, and that these changes affect aerosol dispersion. This study provides support to DOE and NRC regulations that require airflow and CAM placement reevaluations after significant changes in the room. Significant room changes might include variations in ventilation rate and design, large room structure (especially those near supply vents), release locations, sources of heat, and aerosol characteristics (e.g., size).

We found that the addition of room furnishing (for a given ventilation rate) significantly increased lag times, delayed aerosol mixing to remote locations, and increased aerosol dilution. An increase in ventilation rate resulted in a reduction in the lag time and an increase in the air velocities by approximately the same factor as the change in ventilation rate. Secondly, the use of the sonic anemometry and aerosols releases provided useful information for understanding factors controlling the dispersion of aerosols in a test workroom. The collected data set can be used for CFD model validation, a common tool used in workroom ventilation design and analysis. Finally, the results suggest that worker protection could be improved using higher ventilation rates and by having fewer furnishings (more open space) in the room, but this also has to be balanced with operational constraints and the worker's thermal comfort.

Acknowledgments—The authors would like to thank Kenneth R. Alvar, Thomas E. Buhl, John C. Rodgers, Ron C. Scripsick, and Dennis G. Vasilik from Los Alamos National Laboratory and the anonymous reviewers for valuable comments and review of the paper. This work was supported by the U.S. Department of Energy under Contract W7405 ENG-36.

REFERENCES

Awbi, H. B. Ventilation of buildings. London: E&FN Spon Publishers; 1991.

Buchanan, C. R.; Chung, I. P.; Dunn-Rankin, D. A numerical study of indoor contaminant mixing. J. Institute Environmental Sciences 38:15–21; 1995.

Drescher, A. C.; Park, D. Y.; Yost, M. G.; Gadgil, A. J.; Levine, S. P.; Nazaroff, W. W. Stationary and time-dependent indoor tracer-gas concentration profiles measured by OP-FTIR remote sensing and SBFM-computed tomography. Atmospheric Environment 31:727–740; 1997.

Flynn, M. R.; Lackey, B. D.; Muthedath, P. Experimental and numerical studies on the impact of work practices used to control exposures occurring in booth-type hoods. Am. Industrial Hygiene Assoc. J. 57:469–475; 1996.

Haghighat, F.; Huo, Y.; Zang, J.; Shaw, C. The influence of office furniture, workstation layouts, diffuser types, and

location on indoor air quality and thermal comfort conditions at workstations. Indoor Air 6:188–203; 1996.
Hanzawa, H.; Melikov, A. K.; Fanger, P. O. Airflow characteristics in the occupied zone of ventilated spaces. ASHRAE Transactions 93:524–539; 1987.
Heber, A. J.; Boon, C. R. Air velocity characteristics in an experimental livestock building with nonisothermal jet ventilation. ASHRAE Transactions: Symposia 99:1139–1151; 1993.
Hickey, E. E.; Stoetzel, G. A.; Strom, D. J.; Cicotte, G. R.; Wiblin, C. M.; McGuire, S. A. Air sampling in the workplace. Washington, DC: U.S. Nuclear Regulatory Commission; NUREG-1400; 1993.
Hinds, W. C. Aerosol technology: properties, behavior, and measurement of airborne particles. New York: John Wiley and Sons; 1982.
Nicas, M. Estimating exposure intensity in an imperfectly mixed room. Am. Industrial Hygiene Association J. 57:542–550; 1996.
Remington, R. D.; Schork, M. A. Statistics with applications to the biological and health sciences. Englewood Cliffs, NJ: Prentice Hall Inc.; 1970.
Rodgers, J. C.; Whicker, J. J.; Yang, Y.; Moore, M. E.; Gong, H. Optimization of continuous air monitoring (CAM) instrument placement. In: Hoffman, L., ed. Technology development, evaluation, and application (TDEA) FY 1997 progress report. Los Alamos, NM: Los Alamos National Laboratory; Report LA-13438-PR; 1998.
Siurna, D. L.; Bragg, G. M. Stochastic modelling of room air diffusion. Ventilation'85. New York: Elsevier Science Publishers; 1986.
STATISTICA for Windows. Volume I. General conventions and statistics. Tulsa, OK: Statsoft; 1994.
Stull, R. B. An introduction to boundary layer meteorology. Dordrecht, The Netherlands: Kluwer Academic Publishing; 1988.
United States Department of Energy. Air monitoring guide. Washington, DC: U.S. Government Printing Office; U.S. Department of Energy Guide G441.1–8; 1999.
Vogt, R. Intercomparison of ultrasonic anemometers. In: Proceedings of the 12th Symposium on Boundary Layers and Turbulence. Vancouver, BC, Canada: American Meteorological Society; 1997:354–355.
Wasiolek, P. T.; Whicker, J. J.; Gong, H.; Rodgers, J. C. Room airflow studies using sonic anemometry. Indoor Air 9:125–133; 1999a.
Wasiolek, P. T.; Whicker, J. J.; Tavani, R. Influence of room geometry and ventilation rate on airflow and aerosol dispersion. Los Alamos, NM: Los Alamos National Laboratory; Report LA-UR-99-6226; 1999b.
Whicker, J. J. Continuous air monitor correlation to fixed air sample data at Los Alamos National Laboratory. Los Alamos, NM: Los Alamos National Laboratory; Report LA-UR-93-1629; 1993.
Whicker, J. J.; Rodgers, J. C.; Fairchild, C. I.; Scripsick, R. C.; Lopez, R. C. Evaluation of continuous air monitor placement in a plutonium facility. Health Phys. 72:734–743; 1997.
Whicker, J. J.; Rodgers, J. C.; Wasiolek, P. T.; Ammerman, C. N.; Lopez, R. C.; Moore, M. E. Implications of room ventilation and containment design for minimization of worker exposure to plutonium aerosols. Los Alamos, NM: Los Alamos National Laboratory; Report LA-UR-99-5968; 1999.
Whicker, J. J.; Konecni, S.; Parietti, L.; Buhl, T. E.; Hoover, M.; Hoover, P. S.; Martin, R. A.; McAtee, J. L.; Morgan, R. G.; Rodgers, J. C.; Voss, J. T.; Wannigman, D. L. Placement of continuous air monitors in PF-4 laboratories: consensus findings and recommendations. Los Alamos, NM: Los Alamos National Laboratory; Report LA-UR-00-2311; 2000a.
Whicker, J. J.; Baker, G. D.; Wasiolek, P. T. Quantitative measurement of airflow inside a nuclear facility. Health Phys. 79:712–721; 2000b.
Yost, M. G.; Spear, R. C. Measuring indoor airflow patterns by using a sonic vector anemometer. Am. Industrial Hygienist Association J. 53:677–680; 1992.

■ ■